

Article

Energy Relaxation of Porphycene in Atomic and Molecular Cryogenic Matrices

Jacek Dobkowski ¹, Igor V. Sazanovich ^{1,†}, Aleksander Gorski ¹  and Jacek Waluk ^{1,2,*} 

¹ Institute of Physical Chemistry, Polish Academy of Sciences, Kasprzaka 44/52, 01-224 Warsaw, Poland; jdobkowski@ichf.edu.pl (J.D.); igor.sazanovich@stfc.ac.uk (I.V.S.); agorski@ichf.edu.pl (A.G.)

² Faculty of Mathematics and Science, Cardinal Stefan Wyszyński University, Dewajtis 5, 01-815 Warsaw, Poland

* Correspondence: jwaluk@ichf.edu.pl

† Present address: Central Laser Facility, Research Complex at Harwell, STFC Rutherford Appleton Laboratory, Harwell Science and Innovation Campus, Chilton, Oxfordshire OX11 0QX, UK.

Abstract: The kinetics of relaxation of high-lying electronic states of porphycene (porphyrin isomer) embedded in different cryogenic matrices were studied using picosecond time-resolved fluorescence (TRF) and transient absorption (TA) techniques. The molecule was excited into the Soret band, i.e., with a large energy excess compared to that of the lowest (Q) excited state. The TRF and TA time profiles obtained for porphycene embedded in argon and methane matrices were remarkably different: the overall relaxation in argon occurred in 64 ps, whereas the corresponding value for methane matrix was 18 ps. Analysis of the evolution over time of different spectral ranges of TRF spectra indicates the multidimensional character of relaxation kinetics.

Keywords: vibrational relaxation; time-resolved spectra; picosecond transient absorption



Citation: Dobkowski, J.; Sazanovich, I.V.; Gorski, A.; Waluk, J. Energy Relaxation of Porphycene in Atomic and Molecular Cryogenic Matrices. *Photochem* **2022**, *2*, 299–307. <https://doi.org/10.3390/photochem2020021>

Academic Editors: Rui Fausto and Robert Kołos

Received: 1 March 2022

Accepted: 26 March 2022

Published: 6 April 2022

Publisher's Note: MDPI stays neutral with regard to jurisdictional claims in published maps and institutional affiliations.



Copyright: © 2022 by the authors. Licensee MDPI, Basel, Switzerland. This article is an open access article distributed under the terms and conditions of the Creative Commons Attribution (CC BY) license (<https://creativecommons.org/licenses/by/4.0/>).

1. Introduction

When a molecule is electronically excited into a higher-lying state, it undergoes complicated dynamic processes before reaching the thermally equilibrated S_1 level. Energy relaxation involves several intramolecular and intermolecular steps: (i) internal conversion (IC), potentially including intermediate electronic states between the initially excited and the emitting one; (ii) intramolecular vibrational redistribution (IVR); and (iii) thermalization of S_1 , with outflow of energy from the molecule into the environment. These processes usually occur over different timescales. Relaxation dynamics has been intensely studied for porphyrins, which are molecules of biological relevance [1–21]. Excitation into the high-energy Soret band is followed by ultrafast IC (tens to hundreds of femtoseconds), IVR (subpicosecond to single picosecond regime), and cooling (10–20 ps). The relaxation kinetics depends on various factors, such as the structure of the chromophore (e.g., planar vs. nonplanar) or the excess energy acquired via photoexcitation.

Intermolecular relaxation channels are usually slower than intramolecular ones, occurring on the time scale of single to tens of picoseconds in solutions or glasses. However, relaxation can take even longer when the molecule is located in a specific environment, such as cryogenic matrices [22–24]. Under these conditions, relaxation times of several hundred picoseconds have been observed. We have previously demonstrated this by coupling time-resolved fluorescence and transient absorption techniques with matrix isolation. The investigated chromophores included a series of porphyrin isomers—porphycene (Pc, Scheme 1) and its derivatives—embedded in rare gas and nitrogen matrices [25–28]. A large difference in the time-resolved fluorescence profiles was observed for different excitation wavelengths. When the sample was excited using the 355 nm laser line into the Soret band, i.e., with high excess energy (about 11000 cm^{-1} above S_1), fluorescence relaxation occurred

on the time scale of 100 ps. In contrast, for low-energy excitation (593 nm, Q band), the emission was fully relaxed less than 40 picoseconds after photoexcitation [25].



Scheme 1. (Left) porphyrin (porphine); (right) porphycene.

The purpose of the present work is to check to what extent the rate of energy flow from an excited chromophore to the environment can be affected by the structure of the latter. For that purpose, we compared the relaxation kinetics obtained for porphycene in matrices consisting of atoms (Ar) and molecules (CH₄). We observe a clear difference between the relaxation times in the two media. Moreover, the kinetic profiles of the fluorescence evolution strongly depend on the probed spectral range, demonstrating the multidimensional character of the energy relaxation.

2. Materials and Methods

Solid gas matrices were obtained after depositing a stream of gas containing vapors of the investigated compound onto a sapphire window held at 5–30 K in a closed-cycle helium cryostat (Advanced Research Systems Inc., Macungie, PA, USA).

To record the transient absorption (TA) spectra, a home-built pump-probe picosecond spectrometer was used. Pulses with a duration of 1.5 ps (1055 nm) and an energy of 4 mJ, with a repetition of 33 Hz, are provided by a Light Conversion (Vilnius, Lithuania) Nd:glass laser. The third harmonic (352 nm) is used as the pump, whereas the probe, optically delayed with respect to excitation, is the picosecond continuum (400–800 nm) generated in D₂O. The detection unit consists of a Jasný polychromator, containing a Jobin Yvon grating with a flat focusing field, where a CCD matrix is fixed (Hamamatsu S7031, one stage TE-cooled, back-thinned CCD, 1024 × 128 pixels). The temporal resolution of the spectrometer is 2.5 ps.

Time-resolved fluorescence (TRF) spectra were recorded by means of a home-made picosecond spectrofluorimeter, described in detail elsewhere [29]. In short, the first beam (352 nm, 1.5 ps) is used for excitation. The second beam passes through an optical Kerr shutter and opens it. The fluorescence can be transmitted by the shutter only for the time period in which the opening pulse penetrates the Kerr medium. The opening pulse is delayed with respect to the excitation by an optical delay line (maximum delay of 3000 ps, 0.1 ps/step). The delay time is calculated with respect to the maximum of the excitation pulse. The fluorescence is transmitted by a quartz fiber to the detection system consisting of a polychromator (Acton SpectraPro-275, Acton Research Corporation, Acton, MA, USA) and a CCD detector (Princeton Instruments, Inc., Trenton, NJ, USA). The temporal resolution of the spectrofluorimeter is 6.5 ps. The spectra were corrected for the instrumental response.

Time-dependent evolution of TRF spectra can contain artefacts generated by light velocity dispersion (LVD). To check that our results are free from such effects, TRF spectra were recorded for the solution of anthracene in cyclohexane at 294 K. These spectra did not exhibit any differences in the spectral distribution with different delay times. The normalized kinetic curves describing the increased integrated TRF intensity evaluated for spectral intervals of 21,500–25,500, 240,00–25,500, and 21,500–22,700 cm⁻¹ were identical within the margin of experimental error. The increase in the kinetic curves was strictly associated with the temporal resolution of the apparatus.

3. Results and Discussion

3.1. Time-Resolved Fluorescence

The time-resolved fluorescence spectra of porphycene in an Ar matrix are shown in Figure 1. The evolution of the shape of the emission can be clearly observed. Initially (6 ps delay), the spectrum consists of a broad band with the maximum at about $15,600\text{ cm}^{-1}$. At 36 ps delay, it blue shifts by ca. 300 cm^{-1} ; traces of a vibrational structure appear, which become clearly visible after 76 ps. Then, these vibronic features shift to higher energies and become narrower. The fully relaxed spectrum is observed for delay times longer than ca. 150 ps.

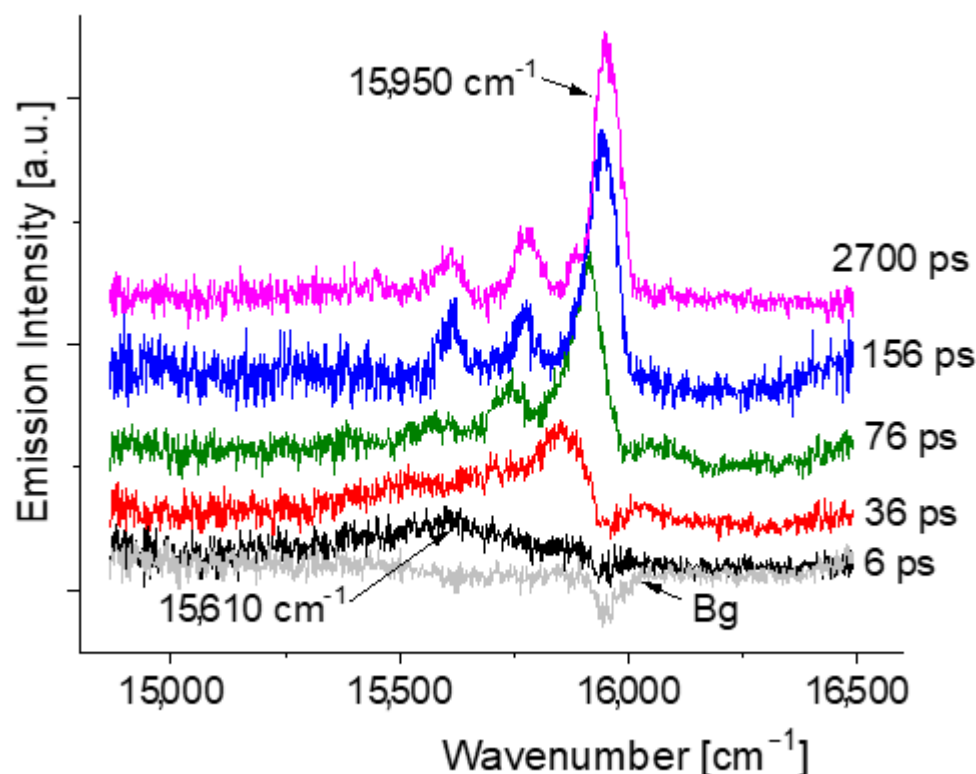


Figure 1. TRF spectra of Pc in argon at 6 K recorded as a function of the delay time: 6, 36, 76, 156, and 2700 ps. The spectra offset was shifted vertically for better visualization. Bg indicates the background.

In our former work [25], time-resolved spectra of the same system at 15 K were recorded, with a time resolution of 30 ps. The present improvement (to 6.5 ps) made it possible to observe changes in the spectral profile occurring during the initial several tens of picoseconds. As shown below, this was crucial for the methane matrices.

We analyzed the kinetic profiles of the spectral changes in emission using two approaches. First, the evolution of the mass center (MC) of the TRF spectra was plotted versus delay time (Figure 2). It could be fitted well with a single exponential risetime of 64 ± 2 ps. In the next step, the evolutions of individual bands were considered separately (Figure 3 and Table 1). The spectral range encompassing the whole emission is labeled P0. P1 corresponds to the 0–0 transition, whereas P2 and P3 denote the features due to the $3A_g$ and $4A_g$ vibrational modes, respectively [30–32]. These totally symmetric modes involve in-plane bending of the pyrrole units. The observed kinetic profiles of integrated intensity are completely different: a biexponential rise is obtained for the integration of the whole emission (P0). In contrast, the low-energy portion (P3) exhibits a rapid rise, followed by a long decay before reaching a plateau (most probably, corresponding to the fluorescence lifetime of about 15 ns). The profile associated with the (0–0) transition (P1) is even more complex, showing an initial delay before the rise, with a time constant similar to

that obtained for the whole emission. These results reflect the multidimensional movement of the initially launched wavepacket.

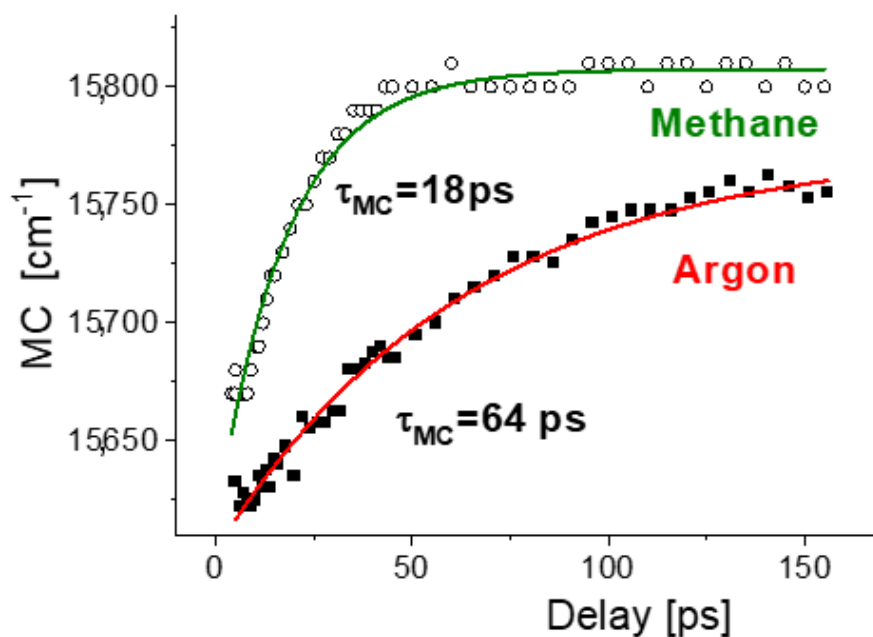


Figure 2. The position of the mass center (MC) of the TRF spectra versus delay time obtained for Pc in argon (squares) and methane (circles) matrices at 6 K and 8 K, respectively. The lines show the results of monoexponential fits: $\tau_{MC} = 64 \pm 2 \text{ ps}$ (argon) and $\tau_{MC} = 18 \pm 2 \text{ ps}$ (methane).

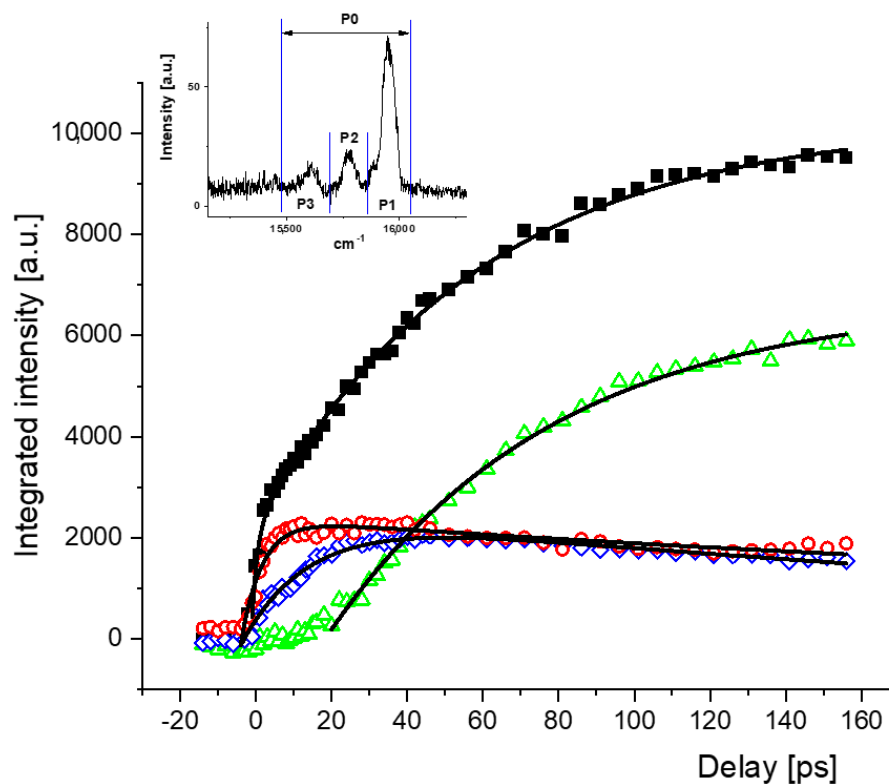


Figure 3. Pc incorporated in argon matrix 6 K. Kinetic profiles of integrated intensity obtained for different integration limits: 15,486–16,029 cm^{-1} (P0, squares), 15,834–16,029 cm^{-1} (P1, triangles), 15,700–15,834 (P2, rhombs), 15,486–15,700 (P3, circles).

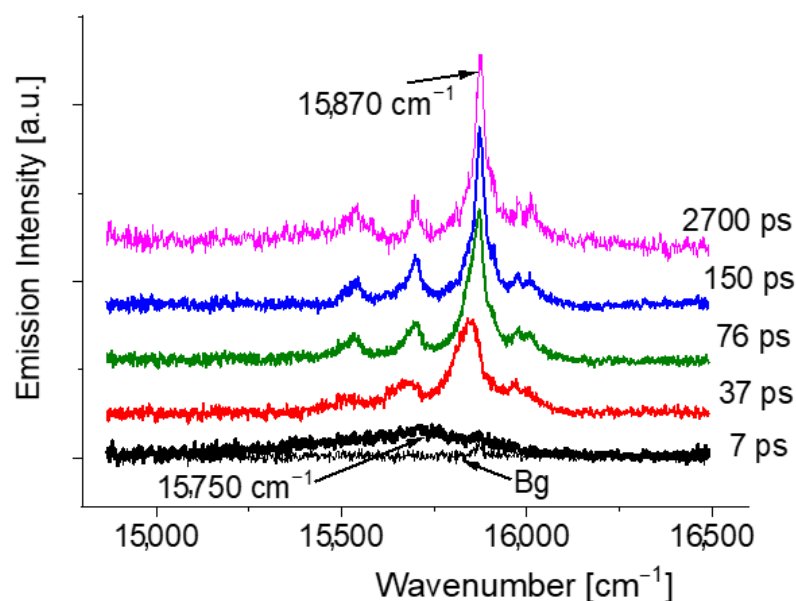
Table 1. Kinetic parameters for Pc incorporated in argon matrix at 6 K, evaluated from the experimental kinetic curves (see Figure 3). D: decay, R: rise.

<Spectral Region>\cm ⁻¹	τ \ps	Amplitude	τ \ps	Amplitude
P0 15,486–16,029	58 ± 2 (R)	8123 ± 80	5 ± 3 (R)	1660 ± 150
P1 15,834–16,029	63 ± 3 (R)	6500 ± 120	-	-
P2 15,700–15,834	18 ± 1 (R)	2680 ± 90	300 ± 31 (D)	2540 ± 100
P3 15,486–15,700	6 ± 0.5 (R)	2474 ± 94	400 ± 45 (D)	2187 ± 47

The same procedures were repeated to analyze the fluorescence of Pc in methane. A shorter relaxation time is evident: the initially (7 ps) broad emission already becomes structured after 37 ps delay, and reaches its final shape at 76 ps (Figure 4). The spectrum recorded after 37 ps delay resembles that in argon obtained after 76 ps. One should also note that the maximum of the broad band observed just after the excitation is separated from the maximum of the relaxed fluorescence by 120 cm⁻¹, whereas the corresponding value for argon was 340 cm⁻¹ (Figure 1). This may be explained by the faster relaxation in CH₄, so that the “initial” spectrum in this matrix is in fact more relaxed than the corresponding spectrum in argon. The evolution of different bands (Figure 5, Table 2) exhibits a pattern similar to that observed for argon: the risetimes increase in the order P3 < P2 < P1; however, the values are definitely shorter for methane. Both P2 and P3 exhibit a decay before reaching a plateau. These decays are about 10 times shorter than in argon.

Table 2. Kinetic parameters for Pc incorporated in methane matrix at 8 K, evaluated from the experimental kinetic curves (see Figure 5). D: decay, R: rise.

<Spectral Region>\cm ⁻¹	τ \ps	Amplitude	τ \ps	Amplitude
P0 15,432–15,952	12 ± 0.4 (R)	10,430 ± 152	1653 ± 321 (D)	10,980 ± 132
P1 15,760–15,952	28 ± 2 (R)	8854 ± 585	380 ± 75 (D)	9072 ± 611
P2 15,606–15,760	8 ± 0.4 (R)	5200 ± 100	24 ± 1 (D)	2761 ± 30
P3 15,432–15,606	5 ± 1 (R)	2560 ± 600	20 ± 7 (D)	1213 ± 640

**Figure 4.** TRF spectra of Pc in methane matrix at 8 K, recorded for different delay times (τ): 7, 37, 76, 150, and 2700 ps. For ease of visualization, the intensity of the spectrum recorded for the delay of 2700 ps was normalized to that of the spectrum recorded for 150 ps. Bg indicates the background.

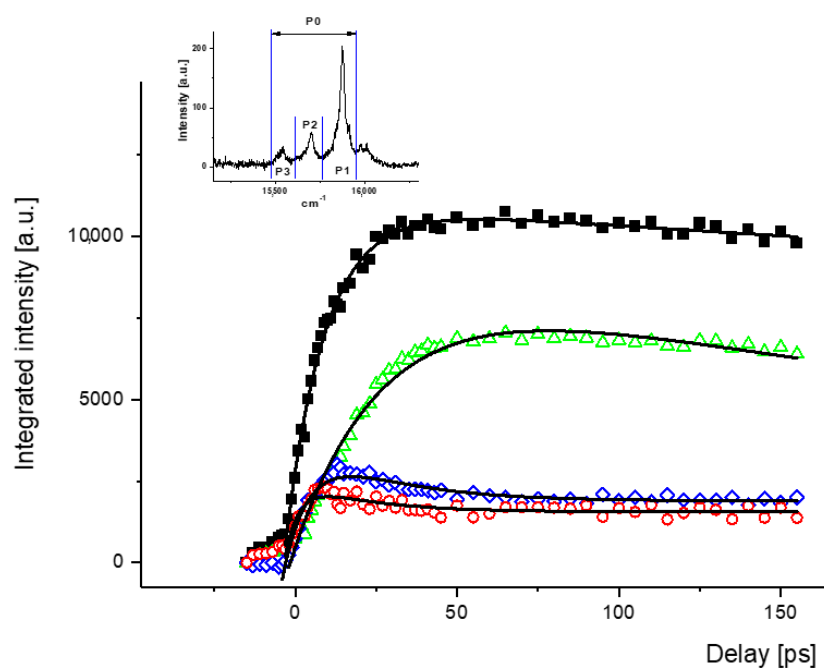


Figure 5. Pc incorporated in methane at 8 K. Kinetics profiles of integrated intensity obtained for different integration limits: (1) 15,432–15,952 cm⁻¹ (P0, squares), 15,760–15,952 cm⁻¹ (P1, triangles), 15,606–15,760 cm⁻¹ (P2, rhombs), and 15,432–15,606 (P3, circles).

3.2. Transient Absorption

An alternative way of probing the relaxation kinetics is to use transient absorption (Figures 6–8). The signal is dominated by ground state bleaching. However, the features P2 and P3, corresponding to 3Ag and 4Ag vibrational modes, appear in the stimulated emission. The kinetic profiles of these bands, indicated by arrows in Figure 6, are in agreement with the data obtained from TRF analysis. Thus, in argon matrix, they are barely visible at a pump-probe delay of 76 ps and become well-structured after 176 ps. In methane, the spectral evolution is faster, so that fully relaxed vibronic features are observed at 76 ps.

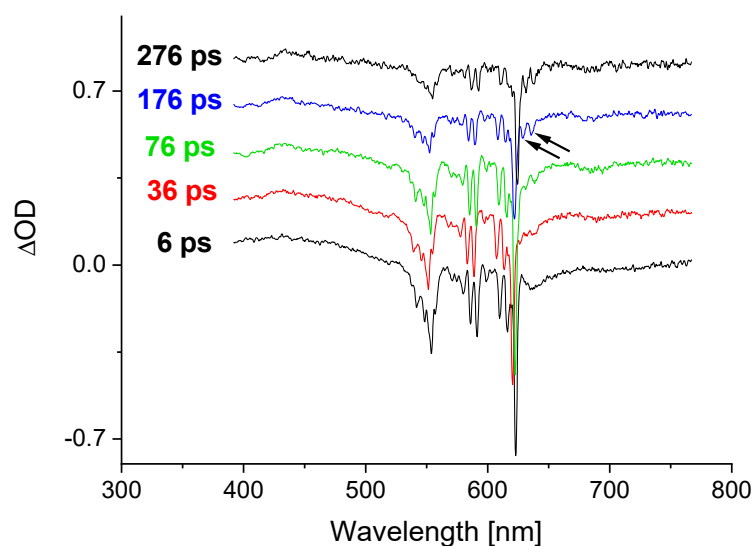


Figure 6. TA spectra of Pc in argon at 6 K recorded as a function of the delay time. The arrows show the vibronic feature of stimulated fluorescence. For ease of visualization, each consecutive spectrum was shifted vertically by 0.2 ΔOD units.

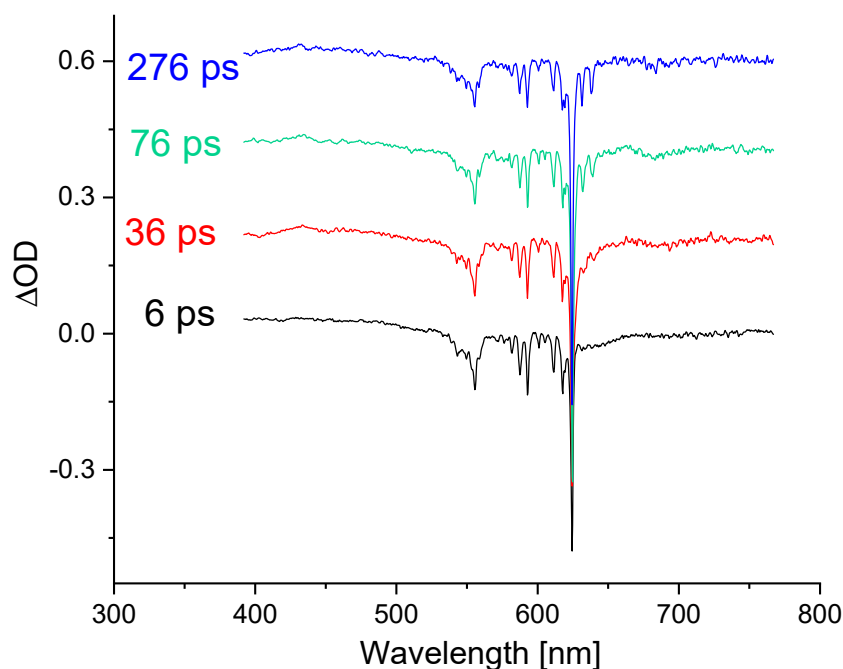


Figure 7. TA spectra of Pc in methane at 30 K recorded as a function of the delay time.

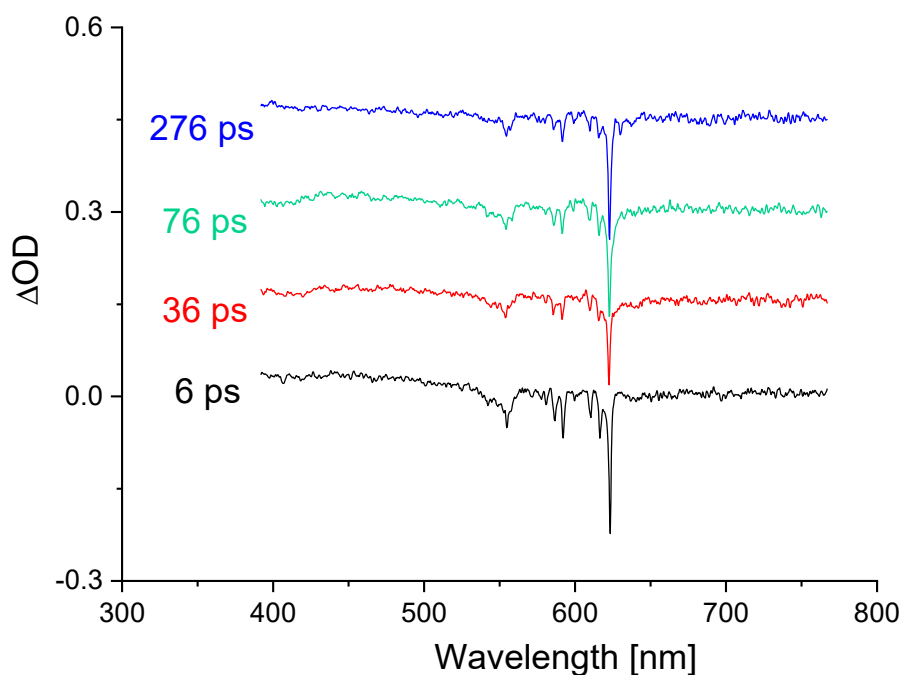


Figure 8. TA spectra of Pc in krypton at 5.2 K recorded as a function of the delay time.

TA spectra were also obtained for Pc embedded in solid krypton (Figure 8). Here, the situation is different: the stimulated emission is practically not observed, except perhaps for very weak signals at 276 ps delay. We attribute the lack of the signal to the heavy atom effect of the matrix, leading to enhanced intersystem crossing to the triplet state, which results in the efficient quenching of fluorescence. Our unpublished data for Pc in xenon reveal nearly 100% triplet formation efficiency.

4. Summary

The time-resolved fluorescence and transient absorption spectra obtained for porphycene embedded in low-temperature argon and methane matrices indicated that S_1

relaxation, involving the outflow of energy from a chromophore photoexcited to high above S_1 , can be as slow as tens or even more than a hundred picoseconds. The relaxation kinetics is significantly dependent on the type of matrix, being considerably faster in solid methane than in argon. At least two factors may be responsible for this difference: (i) the presence of molecular vibrations in methane that can act as energy accepting modes; (ii) the different phonon characteristics of the two matrices. The relaxation kinetics is different for different spectral regions, reflecting the complicated nature of relaxation dynamics. We believe that these experimental data may provide a good starting point for theoretical simulations of intra- and intermolecular energy relaxation processes. What makes porphycene a good candidate for such studies is the fact that the vibrational structure of this molecule is well known for both S_0 and S_1 electronic states [31–33].

Author Contributions: Conceptualization, J.D. and J.W.; investigation, J.D., I.V.S. and A.G.; writing—original draft preparation, J.W.; writing—review and editing, J.D. and A.G. All authors have read and agreed to the published version of the manuscript.

Funding: This work was supported by the Polish National Science Center (grant 2016/22/A/ST4/00029).

Data Availability Statement: Data are contained within the article.

Conflicts of Interest: The authors declare no conflict of interest.

References

1. Baskin, J.S.; Yu, H.Z.; Zewail, A.H. Ultrafast Dynamics of Porphyrins in the Condensed Phase: I. Free Base Tetraphenylporphyrin. *J. Phys. Chem. A* **2002**, *106*, 9837–9844. [[CrossRef](#)]
2. Yu, H.Z.; Baskin, J.S.; Zewail, A.H. Ultrafast Dynamics of Porphyrins in the Condensed Phase: II. Zinc Tetraphenylporphyrin. *J. Phys. Chem. A* **2002**, *106*, 9845–9854. [[CrossRef](#)]
3. Li, X.; Gong, C.; Gurzadyan, G.G.; Gelin, M.F.; Liu, J.; Sun, L. Ultrafast Relaxation Dynamics in Zinc Tetraphenylporphyrin Surface-Mounted Metal Organic Framework. *J. Phys. Chem. C* **2018**, *122*, 50–61. [[CrossRef](#)]
4. Gurzadyan, G.G.; Tran-Thi, T.H.; Gustavsson, T. Time-Resolved Fluorescence Spectroscopy of High-Lying Electronic States of Zn-Tetraphenylporphyrin. *J. Chem. Phys.* **1998**, *108*, 385–388. [[CrossRef](#)]
5. Akimoto, S.; Yamazaki, T.; Yamazaki, I.; Osuka, A. Excitation Relaxation of Zinc and Free-Base Porphyrin Probed by Femtosecond Fluorescence Spectroscopy. *Chem. Phys. Lett.* **1999**, *309*, 177–182. [[CrossRef](#)]
6. Ghosh, M.; Mora, A.K.; Nath, S.; Chandra, A.K.; Hajra, A.; Sinha, S. Photophysics of Soret-Excited Free Base Tetraphenylporphyrin and Its Zinc Analog in Solution. *Spectrochim. Acta A Mol. Biomol. Spectrosc.* **2013**, *116*, 466–472. [[CrossRef](#)]
7. Enescu, M.; Steenkeste, K.; Tfibel, F.; Fontaine-Aupart, M.-P. Femtosecond Relaxation Processes from Upper Excited States of Tetrakis(N-Methyl-4-Pyridyl)Porphyrins Studied by Transient Absorption Spectroscopy. *Phys. Chem. Chem. Phys.* **2002**, *4*, 6092–6099. [[CrossRef](#)]
8. Karolczak, J.; Kowalska, D.; Lukaszewicz, A.; Maciejewski, A.; Steer, R.P. Photophysical Studies of Porphyrins and Metalloporphyrins: Accurate Measurements of Fluorescence Spectra and Fluorescence Quantum Yields for Soret Band Excitation of Zinc Tetraphenylporphyrin. *J. Phys. Chem. A* **2004**, *108*, 4570–4575. [[CrossRef](#)]
9. Lukaszewicz, A.; Karolczak, J.; Kowalska, D.; Maciejewski, A.; Ziolk, M.; Steer, R.P. Photophysical Processes in Electronic States of Zinc Tetraphenyl Porphyrin Accessed on One- and Two-Photon Excitation in the Soret Region. *Chem. Phys.* **2007**, *331*, 359–372. [[CrossRef](#)]
10. Mataga, N.; Shibata, Y.; Chosrowjan, H.; Yoshida, N.; Osuka, A. Internal Conversion and Vibronic Relaxation from Higher Excited Electronic State of Porphyrins: Femtosecond Fluorescence Dynamics Studies. *J. Phys. Chem. B* **2000**, *104*, 4001–4004. [[CrossRef](#)]
11. Liu, X.; Yeow, E.K.L.; Velate, S.; Steer, R.P. Photophysics and Spectroscopy of the Higher Electronic States of Zinc Metalloporphyrins: A Theoretical and Experimental Study. *Phys. Chem. Chem. Phys.* **2006**, *8*, 1298–1309. [[CrossRef](#)] [[PubMed](#)]
12. Venkatesh, Y.; Venkatesan, M.; Ramakrishna, B.; Bangal, P.R. Ultrafast Time-Resolved Emission and Absorption Spectra of Meso-Pyridyl Porphyrins Upon Soret Band Excitation Studied by Fluorescence up-Conversion and Transient Absorption Spectroscopy. *J. Phys. Chem. B* **2016**, *120*, 9410–9421. [[CrossRef](#)] [[PubMed](#)]
13. Rodriguez, J.; Holten, D. Ultrafast Vibrational Dynamics of a Photoexcited Metalloporphyrin. *J. Chem. Phys.* **1989**, *91*, 3525–3531. [[CrossRef](#)]
14. Rodriguez, J.; Kirmaier, C.; Holten, D. Time-Resolved and Static Optical Properties of Vibrationally Excited Porphyrins. *J. Chem. Phys.* **1991**, *94*, 6020–6029. [[CrossRef](#)]
15. Kumble, R.; Palese, S.; Lin, V.S.Y.; Therien, M.J.; Hochstrasser, R.M. Ultrafast Dynamics of Highly Conjugated Porphyrin Arrays. *J. Am. Chem. Soc.* **1998**, *120*, 11489–11498. [[CrossRef](#)]
16. Abraham, B.; Nieto-Pescador, J.; Gundlach, L. Ultrafast Relaxation Dynamics of Photoexcited Zinc-Porphyrin: Electronic-Vibrational Coupling. *J. Phys. Chem. Lett.* **2016**, *7*, 3151–3156. [[CrossRef](#)]

17. Morandeira, A.; Vauthey, E.; Schuwey, A.; Gossauer, A. Ultrafast Excited State Dynamics of Tri- and Hexaporphyrin Arrays. *J. Phys. Chem. A* **2004**, *108*, 5741–5751. [[CrossRef](#)]
18. Kullmann, M.; Hipke, A.; Nuernerger, P.; Bruhn, T.; Götz, D.C.G.; Sekita, M.; Guldi, D.M.; Bringmann, G.; Brixner, T. Ultrafast Exciton Dynamics after Soret- or Q-Band Excitation of a Directly B,B'-Linked Bisporphyrin. *Phys. Chem. Chem. Phys.* **2012**, *14*, 8038–8050. [[CrossRef](#)]
19. Shi, Y.; Liu, J.-Y.; Han, K.-L. Investigation of the Internal Conversion Time of the Chlorophyll a from S_3, S_2 to S_1 . *Chem. Phys. Lett.* **2005**, *410*, 260–263. [[CrossRef](#)]
20. Białkowski, B.; Stepanenko, Y.; Nejbauer, M.; Radzewicz, C.; Waluk, J. The Dynamics and Origin of the Unrelaxed Fluorescence of Free-Base Tetraphenylporphyrin. *J. Photochem. Photobiol. A* **2012**, *234*, 100–106. [[CrossRef](#)]
21. Marcelli, A.; Foggi, P.; Moroni, L.; Gellini, C.; Salvi, P.R. Excited-State Absorption and Ultrafast Relaxation Dynamics of Porphyrin, Diprotonated Porphyrin, and Tetraoxaporphyrin Dication. *J. Phys. Chem. A* **2008**, *112*, 1864–1872. [[CrossRef](#)]
22. Bondybey, V.E.; Milton, S.V.; English, J.H.; Rentzepis, P.M. Spectroscopic and Picosecond Time-Resolved Studies of Vibrational Relaxation in Naphthazarine in Solid Neon. *Chem. Phys. Lett.* **1983**, *97*, 130–134. [[CrossRef](#)]
23. Bondybey, V.E.; Haddon, R.C.; English, J.H. Fluorescence and Phosphorescence of 9-Hydroxyphenalenone in Solid Neon and Its Hydrogen Tunneling Potential Function. *J. Chem. Phys.* **1984**, *80*, 5432–5437. [[CrossRef](#)]
24. Huppert, D.; Bondybey, V.E.; Rentzepis, P.M. Single Excited Vibrational Level Lifetimes and Energy Dissipation Channels of Large Molecules in Inert Matrixes. *J. Phys. Chem.* **1985**, *89*, 5811–5815. [[CrossRef](#)]
25. Dobkowski, J.; Galievsky, V.; Gil, M.; Waluk, J. Time-Resolved Fluorescence Studies of Porphycene Isolated in Low-Temperature Gas Matrices. *Chem. Phys. Lett.* **2004**, *394*, 410–414. [[CrossRef](#)]
26. Dobkowski, J.; Galievsky, V.; Waluk, J. Relaxation in Excited States of Porphycene in Low-Temperature Argon and Nitrogen Matrices. *Chem. Phys. Lett.* **2000**, *318*, 79–84. [[CrossRef](#)]
27. Dobkowski, J.; Lobko, Y.; Gawinkowski, S.; Waluk, J. Energy Relaxation Paths in Matrix-Isolated Excited Molecules: Comparison of Porphycene with Dibenzoporphycenes. *Chem. Phys. Lett.* **2005**, *416*, 128–132. [[CrossRef](#)]
28. Dobkowski, J.; Galievsky, V.; Starukhin, A.; Vogel, E.; Waluk, J. Spectroscopy and Photophysics of Tetraalkyldibenzoporphycenes. *J. Phys. Chem. A* **1998**, *102*, 4966–4971. [[CrossRef](#)]
29. Dobkowski, J.; Galievsky, V.A.; Jasny, J.; Sazanovich, I.V. Time-Resolved Emission Spectroscopy of Pyrene Derivatives. *Pol. J. Chem.* **2004**, *78*, 961–972.
30. Gil, M.; Gorski, A.; Starukhin, A.; Waluk, J. Fluorescence Studies of Porphycene in Various Cryogenic Environments. *Low Temp. Phys.* **2019**, *45*, 656–662. [[CrossRef](#)]
31. Starukhin, A.; Vogel, E.; Waluk, J. Electronic Spectra in Porphycenes in Rare Gas and Nitrogen Matrices. *J. Phys. Chem. A* **1998**, *102*, 9999–10006. [[CrossRef](#)]
32. Gawinkowski, S.; Walewski, Ł.; Vdovin, A.; Slenczka, A.; Rols, S.; Johnson, M.R.; Lesyng, B.; Waluk, J. Vibrations and Hydrogen Bonding in Porphycene. *Phys. Chem. Chem. Phys.* **2012**, *14*, 5489–5503. [[CrossRef](#)] [[PubMed](#)]
33. Mengesha, E.T.; Sepioł, J.; Borowicz, P.; Waluk, J. Vibrations of Porphycene in the S_0 and S_1 Electronic States: Single Vibronic Level Dispersed Fluorescence Study in a Supersonic Jet. *J. Chem. Phys.* **2013**, *138*, 174201. [[CrossRef](#)] [[PubMed](#)]